SAR Signal Penetration Estimation over Ice Sheets and Glaciers Using Multiple Squints and Incoherent Shift Measurements

Akshay Manappatty, Andreas Benedikter, Marc Rodriguez-Cassola, Pau Prats-Iraola, and Gerhard Krieger
Microwaves and Radar Institute, German Aerospace Center (DLR), Germany, andreas.benedikter@dlr.de

Abstract

SAR interferometric elevation measurements of dry snow, firn, and ice are known to be substantially biased downward due to a penetration of the radar signals into the medium. The so-called penetration bias is commonly the main error source in surface elevation measurements over ice sheets. We propose a strategy to estimate the penetration of SAR signals for SAR mission scenarios in which two or more simultaneous or quasi-simultaneous SAR images with different squint angles are acquired, such as for ESA's Harmony mission or the Co-Flier concepts from NASA JPL. The information is inherent in the processed SAR data as phase errors on the azimuth signals resulting from uncompensated non-linear propagation of the radar echoes through the glacial volume. The propagation effects result in almost linear phase errors for squinted acquisitions and hence in a shift of the imaged scene in azimuth direction. By measuring the shift between SAR images acquired with different squint angles, the penetration can potentially be inverted. We evaluate the potential of the approach using simulated SAR acquisitions for the Harmony mission based on real Sentinel-1 imagery.

1 Introduction

The significant penetration of radar signals into snow, firn, and ice at commonly used frequency bands, e.g., from P to X band, results in an elevation bias of the backscatter phase center versus the actual surface, typically described in the literature as penetration bias. In other words, the DEM generated from SAR interferometry (InSAR) data does not replicate the surface, but is biased downward. This bias is commonly the main error source in InSAR surface elevation measurements over ice sheets. Several model-based inversion strategies have been developed to estimate the penetration bias from the interferometric coherence, the backscatter, or both [1, 2, 3]. Those inversion strategies require a detailed modeling of the backscatter distribution, attenuation and permittivity, and are known to result in relevant systematic biases for erroneous model assumptions. In [4], Benedikter et al. propose a penetration estimation approach based on a map-drift autofocus for high-resolution SAR systems that exploits residual phase errors along the synthetic aperture that result from the reduced propagation velocity through the glacial volume. This concept can be applied on single SAR images and does not rely on interferometric information. The benefit of this approach is that only an estimate of the permittivity of the glacial volume is required. However, a sufficient contrast in the imaged scene and a long synthetic aperture are required to have enough sensitivity in the map-drift measurement.

In this paper, we propose to use a similar approach to the one in [4], but applied on multiple simultaneous SAR images with different squint angles. For a squinted acquisition, the penetration into the glacial volume results in almost linear phase errors and hence in a shift of the imaged scene in azimuth direction, where the magnitude of the shift depends on the penetration, the permittivity, and the squint angle. By measuring the shift between SAR images acquired with different squint angles, the penetration can potentially be inverted. ESA's Harmony mission [5] and the Co-Flier concepts from NASA JPL [6] could be perfect candidates to implement the proposed concept, due to the large squint diversity of the constellations. Especially for Harmony that is partially focused on elevation measurements of ice sheets and glaciers, a robust estimation of the penetration bias is highly relevant. The paper is divided as follows. Section 2 outlines the phase error model, Section 3 presents the estimation and inversion approach, Section 4 shows a validation using simulated acquisitions for the Harmony mission, Section 5 provides a discussion on potential limitations, and Section 6 gives a conclusion.

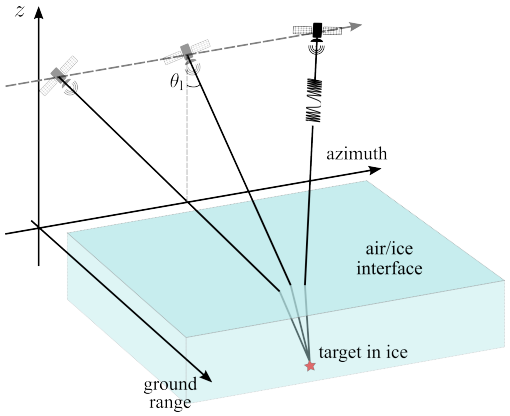

Figure 1 Signal travel paths for different azimuth positions. Note the refraction effect at the surface.

2 Phase Error Due to Squint and Penetration Into the Volume

For a target located within the glacial volume, the reduced propagation velocity within the ice and the refraction at the surface result in an additional signal delay that varies with the azimuth position of the sensor (**Figure 1**). For conventional SAR processing, air is assumed as propagation medium. This results in a phase error along the azimuth dimension between the recorded signal and the SAR focusing kernel. Following [4], the mismatch can be approximated by a Doppler rate error, ΔK_a, that can be written as

$$\begin{aligned}\Delta K_\mathrm{a} &= K_\mathrm{a,ice} - K_\mathrm{a,air} = K_\mathrm{a,air}\cdot\zeta - K_\mathrm{a,air} \\ &= K_\mathrm{a,air}\cdot\left[\frac{\left(H + d\cdot n_\mathrm{ice}\cdot\frac{\cos\theta_\mathrm{i}}{\cos\theta_\mathrm{r}}\right)\cdot n_\mathrm{ice}}{H\cdot n_\mathrm{ice} + d\cdot\frac{\cos\theta_\mathrm{i}}{\cos\theta_\mathrm{r}}} - 1\right],\end{aligned} \tag{1}$$

where $K_\mathrm{a,ice}$ is the correct Doppler rate for a target in ice, $K_\mathrm{a,air}$ is the Doppler rate assumed in processing, ζ descibes the scaling of the Doppler rate for targets in the ice, H the sensor altitude, d the target depth, n_ice the refractive index of the ice as the square-root of the relative permittivity, θ_i the boresight incident angle, and θ_r the corresponding refraction angle that can be derived using Snell's law. We note that ΔK_a is a function of the target depth (i.e., the penetration bias), the refractive index, and the acquisition geometry. The resulting phase error after azimuth focusing along the Doppler band for a squinted acquisition can be approximated as [7]

$$\begin{aligned}\Delta\Phi_\mathrm{a}(f_\mathrm{a}) \approx{}& \pi\cdot\frac{f_\mathrm{DC}}{\sqrt{1-\left(\frac{\lambda\cdot f_\mathrm{DC}}{2\cdot v_\mathrm{e}}\right)^2}}\cdot\frac{\Delta K_\mathrm{a}}{K^2_\mathrm{a,air}} \\ &+ 2\pi\cdot f_\mathrm{DC}\cdot\frac{\Delta K_\mathrm{a}}{K^2_\mathrm{a,air}}\cdot(f_\mathrm{a}-f_\mathrm{DC}) \\ &+ \pi\cdot\frac{\Delta K_\mathrm{a}}{K^2_\mathrm{a,air}}\cdot(f_\mathrm{a}-f_\mathrm{DC})^2,\end{aligned} \tag{2}$$

where f_a is the azimuth frequency, f_DC is the Doppler centroid that is connected to the squint angle, and v_e is the effective velocity of the sensor. The first term in (2) is a bulk phase offset, the second term a linear phase error that results in an azimuth shift of the imaged scene, and the third term a quadratic component that results in defocusing. The defocusing is expected to be negligible for moderate-resolution systems. The azimuth shift of the imaged scene, Δt_a, can be retrieved from the second term in (2) and follows from the Fourier correspondence between a phase ramp in the spectral domain and a shift in the time domain:

$$\Delta t_\mathrm{a} \approx f_\mathrm{DC}\cdot\frac{\Delta K_\mathrm{a}}{K^2_\mathrm{a,air}}. \tag{3}$$

Note that the azimuth shift does not depend on the frequency. **Figure 2** shows the expected azimuth shift for different squint angles and target depths within the glacial volume. A Sentinel-1-like orbit is used and a relative permittivity of 2.5 (corresponding to medium-dense firn) and a boresight incident angle of 35° are assumed. For the roughly 22° squint angle of the Harmony mission, shifts of several meters are to be expected, already for target depths of only few meters. To validate the model, we performed an impulse response function (IRF) simulation for a point target located 8 m deep within a glacial volume with a permittivity of 2.5. The raw data are simulated using a numerical ray-tracing through the volume that can accommodate the propagation effects and the focusing is performed using a time-domain backprojection approach and assuming propagation through air. **Figure 3** shows in red the IRF for an acquisition with zero squint and in green for an acquisition with 20° squint (comparable to the scenario shown in **Figure 4**). The IRFs are shown in a logarithmic scale. A Sentinel-1-like orbit and a frequency of 5.405 GHz are used and an azimuth resolution of 3 m is processed. The skew of the green IRF pattern is a result of the squinted acquisition geometry. Note the clear shift of few meters for the squinted acquisition with respect to the one without a squint.

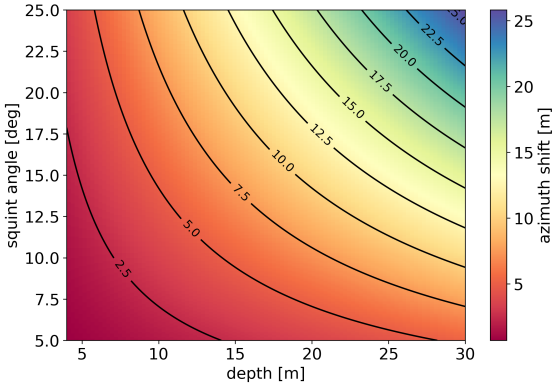

Figure 2 Azimuth shift of the focused scene as a function of the target depth (i.e., the penetration bias) and the squint angle. A Sentinel-1-like orbit is assumed.

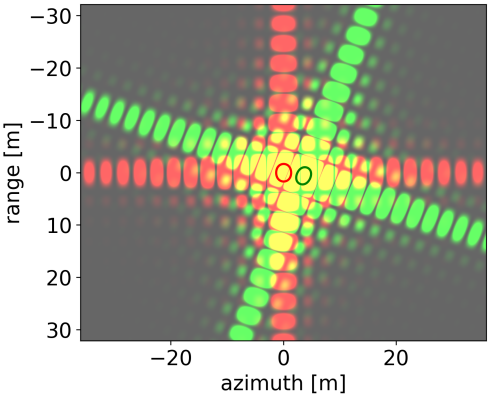

Figure 3 Impulse response function (IRF) simulation for a point target located 8 m deep within a glacial volume with a permittivity of 2.5. The red IRF results for an acquisition with zero squint, the green IRF for an acquisition with 20° squint. The solid lines indicate the −3 dB contour.

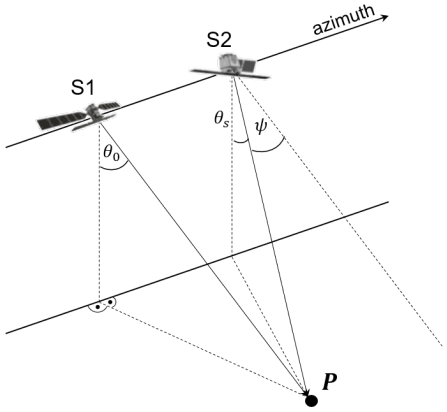

Figure 4 Illustration of the squinted acquisition geometry (S2) compared to a zero-squint acquisition (S1).

3 Inversion Approach

For now we assume a scenario where we acquire two SAR images, S1 and S2, with different squint angles (Figure 4). Inverting the penetration from the shift between the images follows a three-stage approach:

1. SAR processing of both SAR images,
2. block-wise shift estimation between the images,
3. inversion to penetration estimate.

The general procedure is depicted in **Figure 5**. The first stage, SAR processing, describes conventional SAR focusing of the acquired raw data assuming free space propagation. One preliminary assumption of the approach is that nominal calibration has already been applied on the data, to make sure that most of the residual phase signatures are due to the propagation within the glacial volume. In a second stage, the shift between the images is estimated using an incoherent cross-correlation. Sub-pixel accuracy is achieved using an efficient up-sampling procedure of the cross-correlation function. The shift estimation is applied block-wise on the focused data, resulting in a spatially-resolved azimuth shift map over the imaged scene. Finally, the shift map can be inverted to obtain an estimate of the penetration using equations (1) and (3). The accuracy of the measurement scales with the accuracy of the incoherent shift measurement that depends on the contrast in the scene.

4 Simulation for the Harmony Mission

The Harmony constellation consists of two companion satellites to Sentinel-1 as bistatic receivers (**Figure 6**). In the so-called XTI configuration, the two Harmony satellites are forming an across-track interferometer while flying 350 km behind Sentinel-1. This configuration is focused on InSAR elevation measurements over glaciers and ice sheets. There is a squint diversity between the Harmony

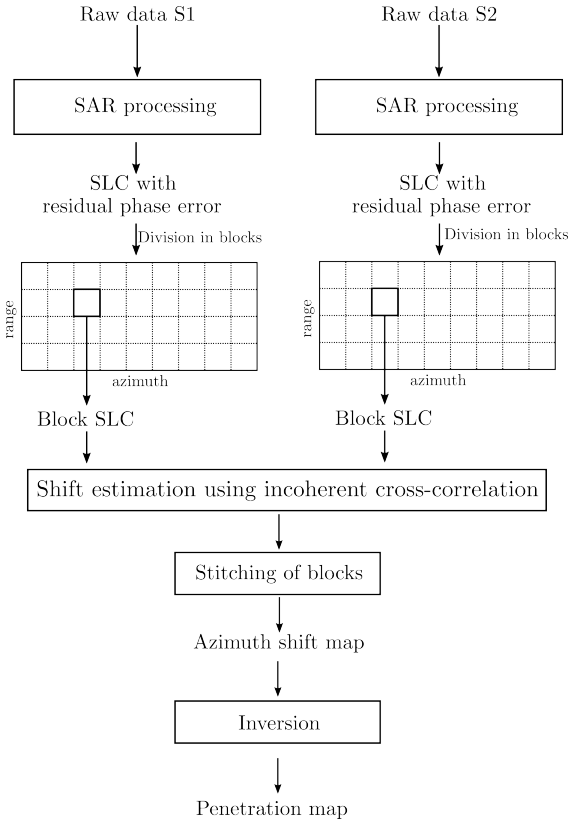

Figure 5 Block diagram of the inversion approach, showing the steps from raw data, over the shift estimation, to the final penetration estimate.

satellites and Sentinel-1 of roughly 22° that can be exploited by applying the proposed inversion approach with shift measurements between the SAR images acquired by Sentinel-1 and the SAR images of the Harmonies. Note again that no interferometric information is used in the inversion approach, it is solely based on an incoherent shift measurement between the SAR images.

We use a Sentinel-1 SAR image acquired over Greenland as basis for the simulation. The quicklook in **Figure 7** indicates the location of the scene. The simulation is performed on a single-look-complex (SLC) level. The results are shown in **Figure 8** for a single burst in the second sub-swath. To generate the SLCs, for both the Sentinel-1 and Harmony acquisition, we use the amplitude images of the real Sentinel-1 scene (Figure 8a) as reflectivity map, multiplied by independent realizations of high-resolution speckle. Figure 8b shows the local incident angles resulting from the geocoding process. Since there is no ground truth of the signal penetration depth, we assume a penetration depth that is varying with the local incident angle between 4 m and 20 m (Figure 8c). A constant permittivity of the ice is assumed. To model the propagation effects on the squinted Harmony acquisition that is flying 350 km behind Sentinel-1, we inject a spatially varying phase error into the spectrum of the Harmony SLC according to the penetration depth map in Figure 8c and the phase error model in (2).

The inversion approach described in Figure 5 is applied on the simulated Sentinel-1 and Harmony SLCs. Figure 8d

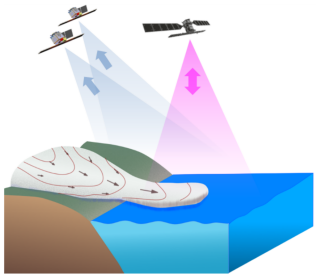

Figure 6 Illustration taken from [8] showing the Harmony constellation in the XTI formation.

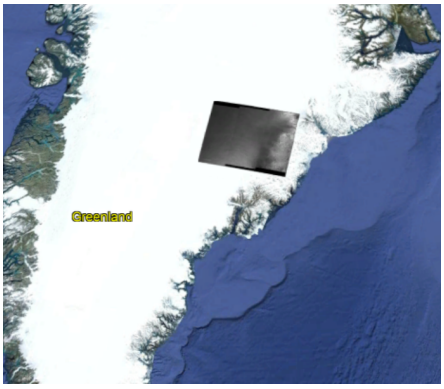

Figure 7 Location of the Sentinel-1 scene used as basis for the simulation.

shows the measured azimuth shifts (in pixels) that show comparable patterns to the depth map. Note that we use overlapping blocks in the shift estimation. The depth d can then be retrieved from the azimuth shifts using the relations in (3) and (1) (Figure 8e). The error between the simulated and the estimated depth is shown in Figure 8f, resulting in a mean error of 6 cm and a standard deviation of 58 cm. Significant errors result in the left portion of the scene, where the variability of the penetration depth is high. The fast varying patterns cannot be perfectly accommodated by the block-based approach. Little errors result in the right portion of the scene that is dominated by low-frequency variations.

5 Short Discussion on Potential Limitations and Error Sources

The proposed approach may be subject to several limitations that are not covered in the rather simple simulation scenario in Section 4 and need to be studied carefully in the future:

- the backscatter of the Sentinel-1 and the Harmony acquisition may be significantly different because of the difference in the squint angle and the bistatic nature of the Harmony acquisition, which will degrade the shift measurement,
- the shift measurement is sensitive to the scene features with the strongest contrast, which may not necessarily correspond to the phase center of the interferometric measurement. Hence, a potential correction of the InSAR penetration would be biased. However, the analyses in [4] show that there is a clear correlation between the shift measurement and the interferometric phase center,
- the shift measurement requires a certain contrast within the scene. SAR acquisitions in the central parts of the big ice sheets show in some areas almost no contrast. This may drastically reduce the accuracy of the shift measurement,
- errors may result for inaccurate estimates of the permittivity of the penetrated volume. Together with coherence-based inversion approaches as described in [1, 2], a joint penetration and permittivity inversion may be possible.

Despite the potential limitations, we believe that the proposed approach may be a valuable source of information (as demonstrated on real data in [4]), especially because it comes for free for mission scenarios like Harmony. Some of the above mentioned points may be constrained by analyzing high-resolution airborne date that may allow to synthesize multiple acquisitions from different portions of the Doppler spectrum with effective squint angles of several degrees.

6 Conclusion

In this paper, a novel approach for estimating the penetration of SAR signals into glaciers and ice sheets based on multiple squints and incoherent shift measurements has been presented. The approach may be used to compensate the InSAR penetration bias in mission scenarios like the ESA's Harmony mission where multiple acquisitions with different squint angles are available. Together with coherence-based approaches as described in [1, 2], a joint penetration and permittivity inversion may be possible.

7 Literature

[1] E. Weber Hoen and H. Zebker, "Penetration depths inferred from interferometric volume decorrelation observed over the Greenland ice sheet," *IEEE Transactions on Geoscience and Remote Sensing*, vol. 38, no. 6, pp. 2571–2583, 2000.

[2] J. Dall, "InSAR elevation bias caused by penetration into uniform volumes," *IEEE Transactions on Geoscience and Remote Sensing*, vol. 45, no. 7, pp. 2319–2324, 2007.

[3] S. Abdullahi, B. Wessel, M. Huber, A. Wendleder, A. Roth, and C. Kuenzer, "Estimating penetration-related X-band InSAR elevation bias: A study over the Greenland ice sheet," *Remote Sensing*, vol. 11, no. 24, 2019.

[4] A. Benedikter, M. Rodriguez-Cassola, F. Betancourt-Payan, G. Krieger, and A. Moreira, "Autofocus-based estimation of penetration depth and permittivity of ice volumes and snow using single SAR images,"

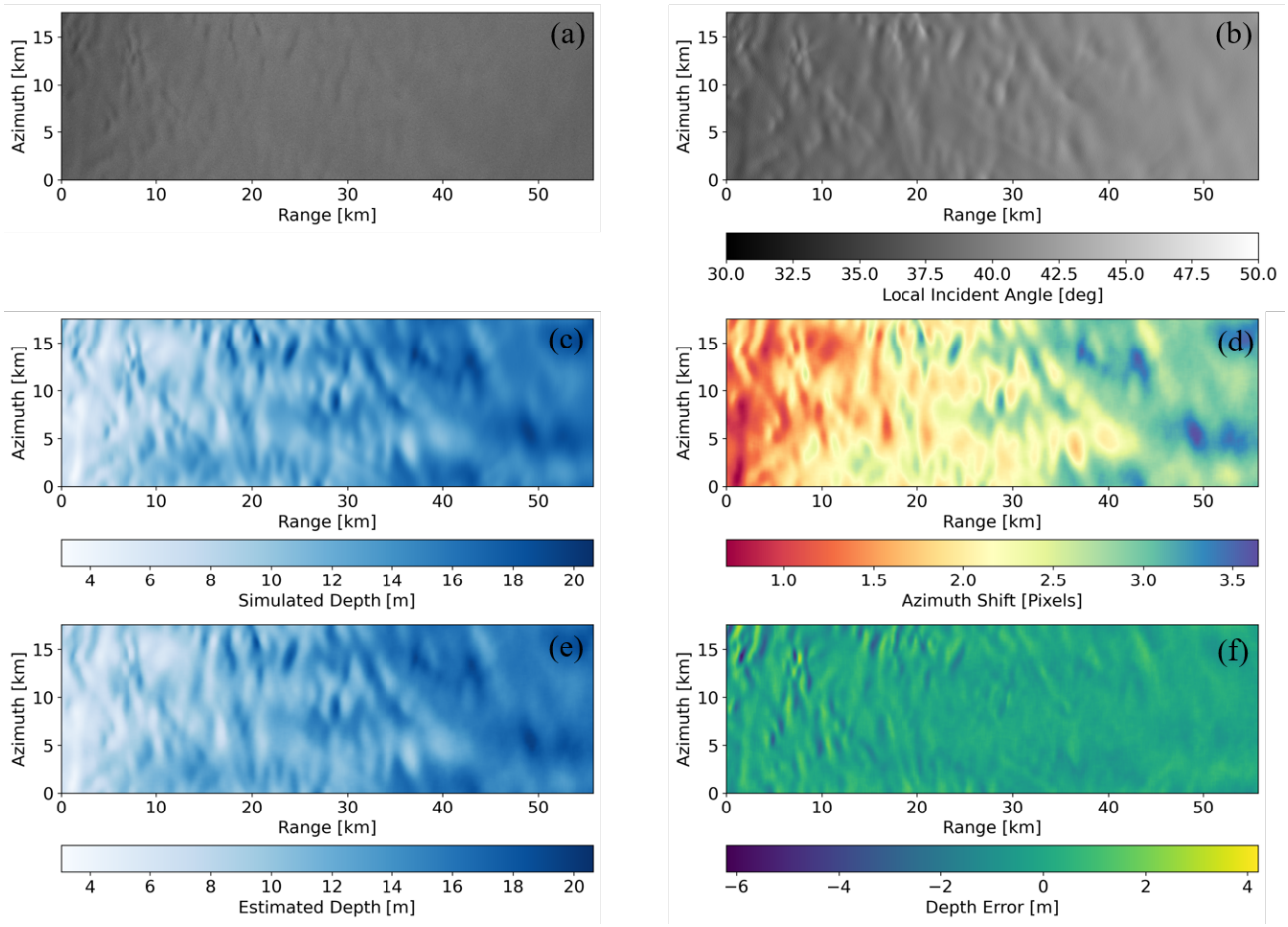

Figure 8 Simulation results based on a real Sentinel-1 acquisition (only one burst is used here) showing: (a) amplitude image of the scene, (b) local incident angles of the Sentinel-1 acquisition, (c) simulated penetration depth map, (d) measured azimuth shift between the Sentinel-1 and Harmony acquisition, (e) estimated penetration depth map inverted from the azimuth shifts, and (f) error between the simulated and estimated penetration depth.

IEEE Transactions on Geoscience and Remote Sensing, vol. 60, pp. 1–15, 2022.

[5] ESA (2022), "Earth Explorer 10 candidate mission Harmony," tech. rep., European Space Agency, Noordwijk, The Netherlands, ESA-EOPSM-HARM-RP-4129, 369pp.

[6] M. Lavalle *et al.*, "Co-fliers concepts formulation for NISAR and ROSE-L to address SDC and STV needs," in *IGARSS 2023 - 2023 IEEE International Geoscience and Remote Sensing Symposium*, 2023.

[7] M. Rodriguez-Cassola *et al.*, "Doppler-related distortions in TOPS SAR Images," *IEEE Transactions on Geoscience and Remote Sensing*, vol. 53, no. 1, pp. 25–35, 2015.

[8] P. López-Dekker *et al.*, "The Harmony mission: End of Phase-0 science overview," in *2021 IEEE International Geoscience and Remote Sensing Symposium IGARSS*, pp. 7752–7755, 2021.